Green synthesis and characterization of silver nanoparticles from the aerial parts of Leucas lanata with enhanced antioxidant and antimicrobial activities

Ruchika Sharma
Shri Guru Ram Rai University
Sheetal Tyagi
Shri Guru Ram Rai University
Indra Rautela
Uttaranchal University
Rakesh Kumar Bachheti
Saveetha Dental College & Hospitals, Saveetha University
Archana Bachheti
Department of Environment Science, Graphic Era (Deemed to be University),
Limenew Abate Worku
limenewabate@gmail.com

Debre Tabor University

Research Article

Keywords: Silver nanoparticles, Green-synthesis, phytochemicals, Capping agents, zeta potential

Posted Date: December 8th, 2025

DOI: https://doi.org/10.21203/rs.3.rs-7981923/v1

Additional Declarations: No competing interests reported.

Version of Record: A version of this preprint was published at Discover Nano on June 28th, 2026. See the published version at https://doi.org/10.1186/s11671-026-04766-5.

Abstract

In the present study, a green, Phyto-assisted approach was employed to synthesize silver nanoparticles (AgNPs) using the aqueous extract of the aerial parts of *Leucas lanata*. The successful formation of AgNPs was evidenced by a characteristic surface plasmon resonance (SPR) band at 384 nm in the UV–Vis absorption spectrum. Elemental mapping and energy-dispersive X-ray (EDX) analysis further confirmed the presence of silver, showing a prominent peak at 2.7 keV. X-ray diffraction (XRD) patterns revealed distinct crystalline planes, which were consistent with the results of Selected area electron diffraction (SAED). High-resolution transmission electron microscopy (HRTEM) determined an average particle size of 25.37 nm. The nanoparticles exhibited a high zeta potential value, suggesting strong stability attributed to phytochemical-mediated capping, as corroborated by Fourier transform infrared spectroscopy (FT-IR). The biosynthesized L-AgNPs displayed potent antioxidant activity with an IC_{50} value of 49 µg/mL in the DPPH assay. L-AgNPs exhibited a higher proportion of ABTS scavenging activity (12.26%) than the *Leucas lanata* extract at a lower concentration of 100 µg/mL, indicating enhanced antioxidant potential. Similarly, the FRAP value of L-AgNPs (21.56 ± 0.17 µM at 100 µg/mL) was significantly greater than that of the aqueous plant extract, further confirming their superior reducing capacity. Moreover, the silver nanoparticles demonstrated significant antimicrobial activity against *Staphylococcus aureus, Escherichia coli, Salmonella abony,* and *Bacillus subtilis.* The MIC value for *Leucas lanata* aqueous extract showed effects between 0.45 and 0.84 mg/mL, whereas L-AgNPs showed effects between 0.09 and 0.34 mg/mL across bacteria. To the best of our knowledge, this is the first report on the silver nanoparticle-synthesizing potential of *Leucas lanata*, highlighting its promising applications in biomedical and pharmaceutical fields.

1. Introduction

Bacterial contamination is a significant cause of various issues in the food industry, medical devices, and water treatment. Both Gram-positive and Gram-negative bacteria are to blame for contamination and many human illnesses. Although many antibacterial agents are available on the market, they harm society due to their side effects, high cost, and toxicity [1, 2]. All these obstacles have been largely overcome by the synthesis of metallic nanoparticles, which are found to be useful in various fields, including electronics, environmental remediation, the medical field, and agriculture (3–5). Metallic nanoparticles can be made from top to bottom and bottom to top. In the top-down method, metallic particles are converted into nanoparticles using various methods, including physical, chemical, and mechanical processes. In contrast, researchers employ physical or chemical vapor deposition, sol-gel, chemical reduction, hydrothermal, solvothermal, spray pyrolysis, laser ablation, and biomimetic techniques to create metallic nanoparticles utilizing the bottom-up strategy [6–9]. The most effective method among these is biomimetic, as it utilizes various microorganisms, enzymes, and plant extracts. In this method, readily available, non-toxic, and inexpensive materials are used to make metallic nanoparticles. Hence, this method is safe for both society and the environment [10–13]. Many silver nanoparticles have been made using the biomimetic method in the biomedical field. Most of these are prepared from plant extracts. Phytochemicals are present in the extracts of various plant parts, including

root, stem, flower, fruit, seed, and leaf. Ag metal nanoparticles of different sizes are made by reducing silver ions [14–19].

In this research, AgNPs have been made from the extract of the *Leucas lanata* plant found in Karnaprayag, Uttarakhand, India, for the first time. *Leucas lanata*, also called woolly leucas, is a soft, densely woolly-haired perennial that grows between 700 and 300 meters above sea level in South India and the Himalayan Mountains. Known by its native name, Gumma or Biskapra, it is a member of the *Lamiaceae family* [20, 21]. In Uttarakhand, people use an extract from the aerial part of the *Leucas lanata* plant to treat a variety of illnesses, including pertussis, stomach, and headaches [21, 22]. While its paste treats wounds, many Uttarakhand residents use its leaves and petals, combined with cold water or milk, to treat illnesses such as colds, coughs, and diarrhea [20]. The *Leucas lanata* plant contains polyphenols, such as protocatechuic acid, caffeic acid, ferulic acid, gallic acid, and chlorogenic acid, according to HPLC studies (Fig. 1) [23].

Silver nanoparticles (AgNPs) synthesized through green methods have gained substantial attention due to their eco-friendly nature, cost-effectiveness, and enhanced biological activities. Various medicinal plants have been employed as reducing and stabilizing agents in the biosynthesis of AgNPs owing to the presence of bioactive phytochemicals [14, 15]. *Leucas lanata*, a traditionally used medicinal herb, is known for its antibacterial, anti-inflammatory, and antioxidant properties [24–26]. Despite its ethnopharmacological significance and rich phytochemical profile, *Leucas lanata* remains underexplored in the context of nanobiotechnology. To date, no comprehensive scientific report is available on the use of the aerial parts of *Leucas lanata* for the green synthesis of AgNPs and their evaluation for antioxidant and antimicrobial activities. This study aims to bridge this knowledge gap by investigating the potential of *Leucas lanata* in the biosynthesis of AgNPs and assessing their biomedical relevance, thereby opening new perspectives in the field of plant-based nanomaterials.

The objective of the current study was to produce, describe, and evaluate the biological activity of silver nanoparticles derived from aerial extract for application in the medical field, given the importance of *Leucas lanata*.

Protocatechuic acid Caffeic acid Ferulic acid

Gallic acid Chlorogenic acid

Figure 1

Some polyphenol structures found in *the Leucas lanata* plant

2. Materials and Methods

2.1. Collection and identification of plant material

The plant material was collected from Karnaprayag, Uttarakhand, India (30.2575° N, 79.2466° E) in October 2022. The collection of plant material was carried out in compliance with applicable local and national regulations, and no specific permits were required. The collection site was not located on protected or Forest land. The plant is collected from private land. A voucher specimen (No. 1203) was deposited at the Botanical Survey of India, Dehradun. The plant was identified as *Leucas lanata* (family Lamiaceae) by Dr. S. K. Singh, Scientist E and Head of the Department, Botanical Survey of India, Dehradun, India. The collection of plant material was carried out in accordance with all applicable local and national regulations.

2.2. Preparation of *Leucas lanata* plant extract

Leucas lanata fresh aerial parts were cleaned twice or three times with tap water before being rinsed with distilled water to remove any dust or other visible particles from the leaves' surface. It took ten to twenty days in May for this aerial portion to dry at room temperature in the shade. After that, the dried plant was finely ground into a powder. Twenty grams of plant powder and 500 mL of water were heated to 60°C for 20 minutes to produce an aqueous extract of the leaves. After filtering the extract using Whatman filter paper No. 1, it was stored at 4°C for subsequent use [27].

2.3. Green Synthesis of AgNPs

To synthesize AgNPs, 1 mL of *Leucas lanata* extract was added individually to 7 mL, 8 mL, 9 mL, 10 mL, and 11 mL of aqueous solutions containing 1 mM (millimolar), 2 mM, 3 mM, 4 mM, and 5 mM AgNO3, respectively. The reaction mixture was centrifuged for 20 minutes at 4000 rpm and then dried at 60°C to produce the AgNPs, which exhibited a dark brown color at 5 mM and 1:10 $AgNO_3$ concentrations.

2.4. Characterization of AgNPs nanoparticle

Using a UV-VIS spectrophotometer (JASCO V-650), the absorbance of AgNPs in ultrapure water was measured. Analysis of the spectra was done between 300 and 600 nm. The essential information regarding the synthesis of AgNPs is provided by the absorption peak at 400–500 nm [28]. AgNPs were found to have FT-IR (Fourier transform infrared) spectra between 4000 and 400 cm-1 (NICOLET 6700, Thermo Fisher Scientific, Germany). AgNPs' purity and percentage composition were examined using EDX (Energy Dispersive X-ray). The phase composition and structural analysis of the generated product were ascertained by utilizing X-ray beam diffraction (XRD, Bruker, D8 Advance, Germany) at room temperature with CuKα (λ = 1.5406 Å and step size = 0.02°) radiation in the scattering angle of 10–80°. The secondary electron mode of field-emission scanning electron microscopy (FE-SEM, Carl Zeiss, Ultra Plus) was used to examine the surface microstructure and grain size of the produced nanoparticles. Energy-dispersive X-ray spectroscopy (EDX), connected to and integrated with the FE-SEM equipment, was used to determine the chemical composition of the representative samples. The diameter of the produced AgNPs was measured, and their shape was determined using HETEM analysis. Ethanol was used to dissolve the material. A thin dispersion drop was put on a "staining mat." A copper grid coated with Lacey carbon was placed within the drop and coated side up. Following approximately 30 minutes

of sonication, the grid was removed, allowed to air-dry for an additional 30 minutes, and then examined using a JEOL 2100 Transmission Electron Microscope.

2.5. Antioxidant properties

Using the DPPH free radical scavenging assay technique, the antioxidant activity of the produced AgNPs was evaluated. In UV-VIS (Ultraviolet-Visible) spectroscopy, the deep violet DPPH solution in methanol exhibits absorption at 517 nm. An electron from an antioxidant causes it to lighten and turn yellow [29, 30]. 1 mL of DPPH alcoholic solution was combined with an equivalent volume of *Leucas lanata* extract or L-AgNPs at varying concentrations, and the mixture was incubated for 30 minutes at room temperature. One common antioxidant is ascorbic acid. 1 mL of methanol was added to the reaction mixture in place of the extract or sample to obtain a control absorption.

The modified FRAP method, as described by Benzie and Strain (1996), was used to perform the FRAP assay. The stock solution consisted of a 20 mM $FeCl_3 \cdot 6H_2O$ solution in distilled water, 300 mM acetate buffer at pH 3.6, and a 10 mM TPTZ (2,4,6-tripyridyl-striazine) solution in 40 mM HCl. Next, $FeCl_3.6H_2O$ (2.5 ml) was combined with acetate buffer (25 ml) and TPTZ (2.5 ml). Prior to use, the solution's temperature was increased to 37°C. Under dark conditions, 150 µL of plant extract and 2.85 mL of FRAP solution were left to react for 30 minutes. At 593 nm, the absorbance was measured. The standard curve, between 100 and 500 µg/mL $FeSO_4$, was linear. The results were compared to ascorbic acid standards and expressed in µM Fe(II)/g dry mass.

According to Ferreira-Santos et al. (2019), the extracts' capacity to scavenge ABTS radicals was evaluated. In 100 milliliters of distilled water, 0.360 grams of 2,2'-azino-bis(3-ethylbenzothiazoline-6-sulfonic acid) diammonium salt were dissolved to create a 7 mM ABTS stock solution. 0.066 g of the salt was dissolved in 100 mL of distilled water to create a 2.45 mM potassium persulfate ($K_2S_2O_8$) solution separately. The 2.45 mM $K_2S_2O_8$ and 7 mM ABTS solutions were mixed in equal quantities (10 mL each) to create the radical cation. The reaction mixture was allowed to sit at room temperature (25 ± 2°C) in the dark for 12 hours to achieve full radical production and absorbance stability.

A UV-Vis spectrophotometer was used to confirm that the working solution had an absorbance of 0.700 ± 0.020 at 734 nm when the resultant concentrated $ABTS^{+\bullet}$ solution was diluted 1:1 (v/v) with absolute ethanol. To perform the antioxidant capacity experiment, *Leucas lanata* extract or L-AgNPs were used at concentrations of 100, 200, 300, 400, and 500 µg/mL. For two hours, the reaction mixtures were allowed to sit at room temperature in the dark. Using spectrophotometry, a drop in absorbance at 734 nm was observed. Appropriate blanks and controls were utilized.

2.6. Antibacterial activity

The antibacterial susceptibility of L-AgNPs against *Salmonella abony*, *Bacillus subtilis*, *Staphylococcus aureus*, and *Escherichia coli* was evaluated using the agar well diffusion method. A sterile glass spreader dipped in the bacterial culture's inoculum suspension was applied to the hardened nutrient agar plates, and the surface of the agar plates was then thoroughly cleaned. After loading the different

concentrations of the produced L-AgNPs solution into the bored wells, the Petri plates were incubated for 24 hours at 37°C to examine the inhibition zone. The assay's standard was streptomycin at 10 µg/mL. The diameter of the inhibitory zone was measured in millimeters and compared to the control [31].

MIC (Minimum Inhibitor Concentration) Assay

A tube dilution approach was used to determine the MIC. The investigated bacterial species were cultured for 24 hours and then diluted using the 0.5 McFarland standard in 10 mL of tryptic soy broth (TSB) to produce an inoculum of 108 CFU mL 1. Neem extracts at a range of strengths, from 5000 g/mL to 10.0 g/mL, were made in a series of culture tubes using DMSO. Each tube received 0.1 mL of the bacterial cell suspension, which was then incubated at 37°C for 24 hours. The development of the inoculum was ascertained by measuring the turbidity of the broth. The lowest extract concentration that inhibited the development of the test organism was known as the minimum inhibitory concentration, or MIC [32, 33].

3. Results and Discussion

3.1. UV-VIS (Ultraviolet-Visible) spectroscopy

The reaction mixture's color shift from light brown to dark brown due to surface plasma resonances was the leading indicator of AgNP production. UV-VIS spectra of the colloidal solution of AgNPs were then taken, in which a peak at 384nm was observed for L-AgNPs, as shown in Fig. 2. This is similar to the AgNPs mediated by the *Fusarium exquisite, Fusarium solani, and Ficus carica* extracts. Several biomolecules and functional groups found in *Leucas lanata* extract facilitate the bio-reduction and capping of synthetic L-AgNPs [34, 35].

3.2. X-ray beam diffraction (XRD) analysis

X-ray diffraction was employed to ascertain the crystalline structure of the bio-synthesised L-AgNPs. Five peaks were found at 38.09°, 44.18°, 64.41°, 77.33°, and 81.44° in the XRD pattern as shown in Fig. 3, which is also represented by the SAED pattern. These peaks correspond to the [1 1 1], [2 0 0], [2 2 0], [3 1 1], and [2 2 2] planes, respectively. This result confirmed the cubic crystalline structure of L-AgNPs, whose basis was demonstrated in Joint Committee of Powder Diffraction Standards file numbers 040783 and 021098, as shown in different research. According to XRD, the size of synthesized L-AgNPs is estimated from the Debye-Scherrer formula, which ranges from 10nm to 75nm, while the average particle size is approximately 25.37nm, which is also vindicated by HRTEM result [36–40].

Figure 3

X-ray beam diffraction pattern of synthesized AgNPs

3.3. EDAX (Energy Dispersive X-ray) analysis

EDAX was used to determine the chemical composition of the biomimetic synthesized L-AgNPs. The absorption peak for silver nanoparticles is generally believed to occur at 2.7 to 3 keV. In Fig. 4, a peak was observed at 2.7 keV, which assures the presence of silver nanoparticles. Apart from this, signals for C and Cl were also obtained in EDX, indicating that the phytochemical present in the extract of *Leucas lanata* is responsible for the reduction of Ag^{+} ions and the stability of AgNPs. The C-Cl group found in the biomolecule of *Leucas lanata* is the reason for the significantly lower level of Cl, which FTIR further verified. These findings are in good agreement with the published research [41–45].

The EDAX tool is also used for element mapping, which provides a digital photograph showing the distribution of elements in the specimen through the color dots. Figure 5 (a), (b), and (c) show the element mapping of C, Ag, and Cl, respectively, while Fig. 5(d) represents the overlay element mapping of all elements presented with their homogenous distribution in the sample [46].

3.4. FESEM (Field emission scanning electron microscopy) analysis

FESEM assessed the surface morphology of L-AgNPs. The image of 100.00kx magnification is shown in Fig. 6, according to which the shape of synthesized L-AgNPs was found to be spherical and rod-like. The aggregation in L-AgNPs is responsible for a rod-like shape; the same results are also visible from the HRTEM image of L-AgNPs [47, 48].

3.5. Fourier Transform Infrared analysis

Fourier Transform Infrared (FTIR) analysis helps determine which functional groups are present in the biomolecules in *Leucas lanata* extract, which is essential for Ag^{+} ion reduction, capping, and stability of AgNPs. Various sharp bands were obtained in FTIR of L-AgNPs between 3900cm^{-1} and 532 cm^{-1} (Fig. 7). The band near 3900 cm^{-1} is due to N-H stretching, while the band at 3492 cm^{-1} is due to O-H stretching vibration, indicating the presence of alcoholic and phenolic groups. The minor band observed in the region of 2917 cm^{-1} is due to C-H stretching in an alkane. The band observed at 2376 cm^{-1} corresponds to the ≡ C-C stretching vibration. The shared band at 1638 cm^{-1} indicates the presence of a C = O or C = C stretching vibration in the aromatic ring. The bands found at 1382 cm^{-1} and 1113 cm^{-1} are due to the C-O, N-H stretching vibration of the amide linkage, while the bands found at 844 cm^{-1} are due to the C-H banding of alkenes. The band at 532 cm^{-1} is attributed to C-Cl or C-Br stretching vibrations, the presence of which has also been confirmed by EDAX. These bands indicate the presence of phytochemicals in the plant extract, which play a vital role in the formation process and act as capping and stabilizing agents [49–58].

3.6. High-resolution transmission electron microscopy analysis

High-resolution transmission electron microscopy (HRTEM) plays a crucial role in determining the morphology, including the size and shape of AgNPs. Figure 8 shows the particles of L-AgNPs at different magnifications. L-AgNPs have a spherical shape, but due to agglomeration, they also have rod-like morphology, which is also confirmed by the FESEM image (Fig. 8a). For the average particle size, a total of 44 L-AgNPs were sampled to get the average particle size, for which the Image J software was used. The particle size of L-AgNPs ranges from 10 nm to 112 nm. However, particles with more than 50nm are very small, and the average particle size is 28.59nm, which is also verified by XRD (Fig. 8e). In the SEAD pattern of synthesized L-AgNPs, eight spots are found that represent specific crystal planes. Figure 8(e) shows eight concentric circles, out of which four are found to be [1 1 1], [2 0 0], [2 2 0], and [3 1 1] planes, which suggest the crystalline nature of L-AgNPs.The interplanar d spacing of 0.15nm for the [2 2 0] plane of L-AgNPs is shown in the figure. 7(f) [2] [59, 60].

3.7. Dynamic Light Scattering (DLS)

The size distribution and zeta potential of L-AgNPs were ascertained by DLS analysis. The zeta potential can be used to assess the stability of AgNPs. The zeta potential gives information about the charge of the phytochemicals acting as capping reagents. The higher the charge on the surface, the greater the repulsion force existing between the synthesized L-AgNPs, due to which the aggregation of L-AgNPs will decrease and the dispersity of nanoparticles will increase in the medium. The zeta potential value of synthesized L-AgNPs was − 25.4mV, as shown in Fig. 9 (a). According to previous research, a voltage of 30 mV is considered the most stable range for nanosuspensions. It also confirms that synthesized L-AgNPs are relatively stable and have a good colloidal nature. In contrast, Fig. 9(b) shows the particle size distribution of L-AgNPs, which shows that particles are of a higher particle size of more than 100 nm as compared to the particle size suggested by XRD and HRTEM. The difference is due to the sample preparation procedure. In the DLS method, the size of L-AgNPs is obtained as the hydrodynamic diameter, which is why the particle size predicted by DLS is higher than predicted by XRD and HRTEM [58–63].

3.8. Antioxidant activity

The antioxidant activity was determined using the DPPH assay. In this case, ascorbic acid was taken as a control. The antioxidant activity of ascorbic acid, *Leucas lanata* plant extract, and silver nanoparticles made from *Leucas lanata* is completely dose-dependent towards free radicals like DPPH, as shown in Fig. 10(a). The scavenging activity of DPPH of plant extract was lower than that of synthesized L-AgNPs and almost equal to that of ascorbic acid at a high concentration of 500µg/ml. The %RAS values for the plant extract and L-AgNPs at 100 µg/ml were 38% and 45%, respectively. For a maximum concentration of 500 µg/ml, the %RAS values were 81% and 93%, respectively. The IC_{50} value for the plant extract of

Leucas lanata was 154 µg/ml, whereas for L-AgNPs, it was found to be 49 µg/ml, as shown in Fig. 10(b), which is significantly lower compared to the *Leucas lanata* plant extract. This result is also confirmed by results obtained for silver nanoparticles mediated by *Cucumis prophetarum* [64–66]. *The* aqueous extract of Leucas lanata and L-AgNPs demonstrated their ABTS radical scavenging activity in Fig. 10(c). When compared to aqueous plant extract, L-AgNPs exhibit a larger proportion of ABTS scavenging activity. At lower concentrations of 100 µg/ml, L-AgNPs exhibit 12.26% inhibition, whereas at higher concentrations of 500 µg/ml, they exhibit 59.92% inhibition. Nonetheless, the plant's aqueous extract exhibits 8.75% at lower concentrations of 100 µg/ml and 53.17% at higher concentrations of 500 µg/ml. Figure 10(d) showed the FRAP assay of L-AgNPs and the aqueous extract of *Leucas lanata*. L-AgNPs have a higher FRAP than aqueous plant extract. L-AgNPs show 21.56 ± 0.17 µM at a lower concentration of 100 µg/ml and 83.31 ± 0.15 µM at higher values of 500 µg/ml. However, at a lower concentration of 100 µg/ml, the aqueous solution of the plant extract shows 14.29 ± 0.11, whereas at a higher concentration of 500 µg/ml, it shows 69.54 ± 0.21. The current findings showed that, in addition to silver nanoparticles exhibited potent antioxidant activity compared with aqueous plant extract of *Leucas lanata*, as previously supported by the previous study [67–69]

Fig: 10(a): DPPH (2,2-Diphenyl-1-picrylhydrazyl) assay analysis for Antioxidant activity

Figure 10(b): DPPH (2,2-Diphenyl-1-picrylhydrazyl) Free radical scavenging Activity AgNPs and IC_{50} values

3.9. Antibacterial Activity

The antibacterial activity of, was tested using two gram-positive and two gram-negative pathogens: *Salmonella ebony*, *Bacillus subtilis, Escherichia coli*, and *Staphylococcus aureus* as positive and negative controls, respectively, streptomycin and All Bacteria culture diluted 10^8 CFU/ml and spread on agar plate for incubation 24 hr at 37ºC to measure the inhibition zones. DMSO were employed as observed Fig. 11 and Fig. 12. The activity of the produced L-AgNPs against gram-positive and gram-negative bacteria was nearly identical. Silver nanoparticles derived from the peel of *Citus sinensis* and *Acacia leucophloea* also showed comparable outcomes [70, 71]. The table displays the inhibition zone at various concentrations. Compared to L-AgNPs, the inhibitory zone of the plant extract is smaller. At the lowest concentration of L-AgNPs, *Bacillus subtilis* exhibited the highest inhibitory zone, measuring 10 mm (Table 1). When bacteria and silver ions interact, it inhibits essential processes such as DNA replication, respiratory enzyme function, and ATP synthesis, ultimately leading to cell death [72–73].

Table 1
Inhibition Zone Diameter(mm) for different Bacteria

Concentration	*Staphylococcus aureus(P)*		*Escherichia coli(Q)*		*Salmonella abony(R)*		*Bacillus subtilis (S)*	
	***Leucas lanata* Plant extract**	**L-AgNPs**	***Leucas lanata* Plant extract**	**L-AgNPs**	***Leucas lanata* Plant extract**	**L-AgNPs**	***Leucas lanata* Plant extract**	**L-AgNPs**
2000µg/mL (A)	6 mm	20mm	10 mm	25mm	10 mm	17mm	16 mm	20mm
1000µg/mL (B)	4 mm	10 mm	6 mm	19mm	4mm	12mm	6 mm	15mm
500µg/mL (C)	---------	5 mm	--------	11mm	--------	8mm	-------	12mm
250µg/mL (D)	--------	-------	--------	6mm	-------	------	---------	10mm
Streptomycin µg/mL(F) Positive Control	20 mm	23 mm	24 mm	29mm	20 mm	20mm	20mm	23mm
DMSO (Dimethyl sulfoxide) (E) (Negative Control)	--------	-------	--------	-------	--------	-------	--------	-------

MIC (Minimum Inhibitory Concentration) against Bacteria

Figure 13 shows that the aqueous extract of Leucas lanata exhibited effects between 0.45 and 0.84 mg/mL, whereas L-AgNPs showed effects between 0.09 and 0.34 mg/mL across the bacteria. With a minimum inhibitory concentration (MIC) of 0.84 mg/mL, the plant extract in aqueous solution showed the most potent effects against *Salmonella abony*. *Bacillus subtilis* was inhibited with a minimum inhibitory concentration (MIC) of 0.76 mg/mL, whereas *E.coli* showed the strongest action with the lowest MIC value of 0.45 mg/mL. MIC 0.68 mg/ml is moderate for *Staphylococcus aureus*. With a minimum inhibitory concentration (MIC) of 0.09 mg/mL, L-AgNPs exhibited the most notable efficacy against *E. coli*. The MIC value for the second activity against *Staphylococcus aureus* was 0.16 mg/mL. *Bacillus subtilis* and *Salmonella abony*, on the other hand, exhibit 0.34 and 0.24 mg/ml, respectively. Consequently, L-AgNPs exhibit a MIC value that is noticeably higher than that of the plant's aqueous extract.

4. Limitations and Future Scope of the Study

The study has some limitations that warrant further investigation. The exact mechanism by which phytochemicals interact to stabilize and cap the silver nanoparticles was not fully elucidated, leaving a gap in understanding the underlying processes. The antimicrobial activity was evaluated against a limited number of bacterial strains; expanding the investigation to include a broader range of microorganisms, such as fungi and drug-resistant strains, would provide more comprehensive insights into the efficacy of the nanoparticles. Additionally, the environmental impact of *Leucas lanata*-based silver nanoparticles, including their biodegradability and long-term stability within ecological systems, remains unexplored. The absence of in vivo studies to validate the in vitro antioxidant and antimicrobial efficacy represents another limitation, as such studies are critical for practical and clinical applications. Addressing these limitations in future research would significantly enhance the relevance and applicability of the study.

5. Conclusion

Several biological entities have recently been investigated for their ability to mediate the green synthesis of silver nanoparticles (AgNPs). In this study, *Leucas lanata* extract, prepared from its aerial parts, was employed as a natural reducing and capping agent for the synthesis of AgNPs. Characterization techniques, such as UV-VIS spectroscopy, confirmed nanoparticle formation with a distinct absorption peak at 384 nm, while EDX analysis verified the elemental composition of the silver. Morphological assessment using HRTEM and structural evaluation through XRD indicated that the L-AgNPs were predominantly spherical with an average particle diameter of under 29 nm. The antioxidant capacity of the synthesized nanoparticles was evaluated using the DPPH, ABTS, and FRAP radical scavenging methods, which suggest an enhanced antioxidant efficiency of L-AgNPs. The antibacterial efficacy of L-AgNPs was tested against two Gram-positive *(Staphylococcus aureus, Bacillus subtilis)* and two Gram-negative *(Escherichia coli, Salmonella abony)* strains. L-AgNPs exhibit a MIC value that is noticeably higher than that of the plant's aqueous extract. Results demonstrated consistent inhibitory zones across all four bacterial species, with a slightly higher zone of inhibition observed against *Bacillus subtilis*. These findings highlight the effectiveness of *Leucas lanata* as a novel, eco-friendly source for the synthesis of bio-functional silver nanoparticles with promising antimicrobial and antioxidant properties.

Abbreviations

SPR
Surface plasmon resonance
AgNPs
Silver Nanoparticles,
UV-VIS
Ultraviolet- Visible
EDX
Energy Dispersive X-ray
XRD

X-ray beam diffraction,
FTIR
Fourier Transform Infrared
FESEM
Field emission scanning electron microscopy
HRTEM
High-resolution transmission electron microscopy
DPPH
2,2-Diphenyl-1-picrylhydrazyl
mM
millimolar
JCPDS
Joint Committee on Powder Diffraction Standards
SAED
Selected area electron diffraction
DMSO
Dimethyl sulfoxide and L-AgNPs:Silver nanoparticles mediated by *Leucas lanata* extract
℃
Degree Celsius
mm
millimetre
gm
gram:FRAP:Ferric Reducing Antioxidant Power TPTZ:2,4,6-tripyridyl-striazine
ABTS
2,2'-azino-bis-(3-ethylbenzothiazoline-6-sulfonic acid)
MIC
Minimum Inhibitory Concentration
CFU
Colony-Forming Unit

Declarations

Author Contributions Statement: "R.S., S.T., and I. R. wrote the main manuscript text, and R.K.B. A.B. and L.A.W. prepared different tables and figures. All authors reviewed the manuscript."

Funding Statement: This research received no specific grant from any funding agency in any sectors.

Data Availability: All relevant data are within the manuscript

Declarations

Ethics, consent to participate, and consent to publish

Not applicable.

Ethics declaration

Not applicable.

Clinical trial number

Not applicable.

Competing interests

The authors declare no competing interests.

References

1. Ameen F, Srinivasan P, Selvankumar T, Kamala-Kannan S, Al Nadhari S, Almansob A, Govarthanan M (2019) Phytosynthesis of silver nanoparticles using Mangifera indica flower extract as bioreductant and their broad-spectrum antibacterial activity. Bioorg Chem 88:102970. https://doi.org/10.1016/j.bioorg.2019.102970
2. Rana A, Kumari A, Chaudhary AK, Srivastava R, Kamil D, Vashishtha P, Sharma SN (2023) An investigation of antimicrobial activity for plant pathogens by green-synthesized silver nanoparticles using Azadirachta indica and Mangifera indica. Physchem 3(1):125–146. https://doi.org/10.3390/physchem3010010
3. Mittal AK, Kaler A, Banerjee UC (2012) Free Radical Scavenging and Antioxidant Activity of Silver Nanoparticles Synthesized from Flower Extract of Rhododendron dauricum. Nano Biomed Eng 4(3):1–7. https://doi.org/10.5101/nbe.v4i3.p1-7
4. Sharma R, Kandwal A, Tyagi S (2023) Plant-mediated Green Synthesis of Silver Nanoparticles and its Biomedical Applications: A Review. J Environ Biosci 37(1):1–10
5. Padilla-Camberos E, Sanchez-Hernandez IM, Torres-Gonzalez OR, Ramirez-Rodriguez P, Diaz E, Wille H, Flores-Fernandez JM (2021) Biosynthesis of silver nanoparticles using *Stenocereus queretaroensis* fruit peel extract: Study of antimicrobial activity. Materials 14(16):4543. https://doi.org/10.3390/ma14164543
6. Jamkhande PG, Ghule NW, Bamer AH, Kalaskar MG (2019) Metal nanoparticles synthesis: An overview on methods of preparation, advantages and disadvantages, and applications. J Drug Deliv Sci Technol 53:101174. https://doi.org/10.1016/j.jddst.2019.101174
7. Ndlomingo MJ, Bingwa N, Meijboom R (2020) Review of supported metal nanoparticles: synthesis methodologies, advantages and application as catalysts. J Mater Sci 55(15):6195–6241. https://doi.org/10.1007/s10853-020-04556-2
8. Habibullah G, Viktorova J, Ruml T (2021) Current strategies for noble metal nanoparticle synthesis. Nanoscale Res Lett 16(1):47. https://doi.org/10.1186/s11671-021-03507-5

9. Shnoudeh AJ, Hamad I, Abdo RW, Qadumii L, Jaber AY, Surchi HS, Alkelany SZ (2019) Synthesis, characterization, and applications of metal nanoparticles. In: Biomaterials and bionanotechnology. Academic Press; pp. 527–612. https://doi.org/10.1016/B978-0-12-814427-5.00019-2
10. Shah M, Fawcett D, Sharma S, Tripathy SK, Poinern GEJ (2015) Green synthesis of metallic nanoparticles via biological entities. Materials 8(11):7278–7308. https://doi.org/10.3390/ma8115377
11. Yadi M, Mostafavi E, Saleh B, Davaran S, Aliyeva I, Khalilov R, Milani M (2018) Current developments in green synthesis of metallic nanoparticles using plant extracts: a review. Artif Cells Nanomed Biotechnol 46(sup3):336–343. https://doi.org/10.1080/21691401.2018.1457036
12. Dikshit PK, Kumar J, Das AK, Sadhu S, Sharma S, Singh S, Kim BS (2021) Green synthesis of metallic nanoparticles: Applications and limitations. Catalysts 11(8):902. https://doi.org/10.3390/catal11080902
13. Vijayaram S, Razafindralambo H, Sun YZ, Vasantharaj S, Ghafarifarsani H, Hoseinifar SH, Raeeszadeh M (2024) Applications of green synthesized metal nanoparticles—a review. Biol Trace Elem Res 202(1):360–386. https://doi.org/10.1007/s12011-023-03705-9
14. Kumar B, Smita K, Cumbal L, Debut A (2017) Green synthesis of silver nanoparticles using Andean blackberry fruit extract. Saudi J Biol Sci 24(1):45–50. https://doi.org/10.1016/j.sjbs.2016.02.025
15. Iravani S, Zolfaghari B (2013) Green synthesis of silver nanoparticles using Pinus eldarica bark extract. BioMed Res Int 2013:639725. https://doi.org/10.1155/2013/639725
16. Jagtap UB, Bapat VA (2013) Green synthesis of silver nanoparticles using Artocarpus heterophyllus Lam. seed extract and its antibacterial activity. Ind Crops Prod 46:132–137. https://doi.org/10.1016/j.indcrop.2013.01.034
17. Mohammadi F, Yousefi M, Ghahremanzadeh R (2019) Green synthesis, characterization and antimicrobial activity of silver nanoparticles (AgNPs) using leaves and stems extract of some plants. Adv J Chem Sect A 2(4):266–275
18. Nagaraja SK, Niazi SK, Bepari A, Assiri RA, Nayaka S (2022) Leonotis nepetifolia flower bud extract mediated green synthesis of silver nanoparticles, their characterization, and in vitro evaluation of biological applications. Materials 15(24):8990. https://doi.org/10.3390/ma15248990
19. Ram GD, Kumar SP, Srinivasan TK, Aravind T, Ramya S, Lingaraja D, Bhuvaneshwari G (2023) Green synthesis of silver nanoparticles using Chrysopogon zizanioides root extract and their antibacterial activities. Mater Today Proc. https://doi.org/10.1016/j.matpr.2023.05.026
20. Dixit V, Verma P, Agnihotri P, Paliwal AK, Rao CV, Husain T (2015) Antimicrobial, antioxidant and wound healing properties of Leucas lanata Wall. ex Benth. J Phytopharmacol 4(1):9–16
21. Pala NA, Negi AK, Gokhale Y, Todaria NP (2011) Species composition and phytosociological status of Chanderbadni sacred forest in Garhwal Himalaya Uttarakhand India. NeBIO 2:52–59
22. Verma R, Tapwal A, Kumar D, Puria S (2020) Phytochemical profiling and biological activity of Leucas lanata Benth. an important ethnomedicinal plant of Western Himalaya. Ecol Environ Conserv 26:169–175

23. Ramalingam R, Nath AR, Madhavi BB, Nagulu M, Balasubramaniam A (2013) Free radical scavenging and antiepileptic activity of Leucas lanata. J Pharm Res 6(3):368–372
24. Selahuddeen ML, Salleh NAFM, Lee FL, Manisekaran H, Bouguerra MDE, Samsudin WNAWM, Abdullah F (2024) Phytochemical Attributes and Pharmacological Activities of Genus Leucas: A Mini Review. J Mater Life Sci. ;58–74
25. Sharma R, Tyagi S, Sati SC Green Synthesis, Characterization And Antioxidant Activity Of ZnO Nanoparticles Mediated By Aerial Parts Of Leucas lanata. (No journal specified in original; assumed as presented).
26. Champati BB, Jena S, Ray A, Mohanty S, Sahoo A, Das PK, Panda PC (2023) Chemical Composition and Antioxidant Activity of Essential Oil of Leucas lanata. Chem Nat Compd 59(2):386–388. https://doi.org/10.1007/s10600-023-04102-7
27. Vijayakumar S, Mahadevan S, Arulmozhi P, Sriram S, Praseetha PK (2018) Green synthesis of zinc oxide nanoparticles using Atalantia monophylla leaf extracts: Characterization and antimicrobial analysis. Mater Sci Semicond Process 82:39–45. https://doi.org/10.1016/j.mssp.2018.03.024
28. Peron S, Hadi F, Azarbani F, Ananda Murthy HC (2021) Antimicrobial, antioxidant, anti-glycation and toxicity studies on silver nanoparticles synthesized using Rosa damascena flower extract. Green Chem Lett Rev 14(3):519–533. https://doi.org/10.1080/17518253.2021.1949168
29. Flieger J, Franus W, Panek R, Szymańska-Chargot M, Flieger W, Flieger M, Kołodziej P (2021) Green synthesis of silver nanoparticles using natural extracts with proven antioxidant activity. Molecules 26(16):4986. https://doi.org/10.3390/molecules26164986
30. Ravichandran V, Vasanthi S, Shalini S, Shah SAA, Harish R (2016) Green synthesis of silver nanoparticles using Atrocarpus altilis leaf extract and the study of their antimicrobial and antioxidant activity. Mater Lett 180:264–267. https://doi.org/10.1016/j.matlet.2016.05.108
31. Hasan KF, Horváth PG, Horváth A, Alpár T (2021) Coloration of woven glass fabric using biosynthesized silver nanoparticles from Fraxinus excelsior tree flower. Inorg Chem Commun 126:108477. https://doi.org/10.1016/j.inoche.2021.108477
32. Marrez DA, Naguib MM, Sultan YY, Higazy AM (2019) Antimicrobial and anticancer activities of Scenedesmus obliquus metabolites. Heliyon 5(3):e01372. https://doi.org/10.1016/j.heliyon.2019.e01372
33. Wiegand I, Hilpert K, Hancock REW (2008) Agar and broth dilution methods to determine the minimal inhibitory concentration (MIC) of antimicrobial substances. Nat Protoc 3(2):163–175. https://doi.org/10.1038/nprot.2007.521
34. Saha P, Rajkumar K, Abraham J (2012) Comparative study on antimicrobial property of silver nanoparticles synthesized by Fusarium equiseti and Fusarium solani. J Bionanosci 6(1):28–32. https://doi.org/10.1166/jbns.2012.1017
35. Ulug B, Turkdemir MH, Cicek A, Mete A (2015) Role of irradiation in the green synthesis of silver nanoparticles mediated by fig (Ficus carica) leaf extract. Spectrochim Acta Mol Biomol Spectrosc 135:153–161. https://doi.org/10.1016/j.saa.2014.06.130

36. Singha S, Neog K, Kalita PP, Talukdar N, Sarma MP (2014) Biological synthesis of silver nanoparticles by Neptunia oleraceae. Int J Basic Appl Biol 2(2):55–59
37. Abdullah NISB, Ahmad MB, Shameli K (2015) Biosynthesis of silver nanoparticles using Artocarpus elasticus stem bark extract. Chem Cent J 9:1. https://doi.org/10.1186/s13065-014-0089-6
38. Doan VD, Nguyen TD, Nguyen TLH, Nguyen HT (2019) Green synthesis of silver nanoparticles using aganonerion polymorphum leaves extract and evaluation of their antibacterial and catalytic activity. Mater Res Express 6(11):1150g1. https://doi.org/10.1088/2053-1591/ab4e8b
39. Bidian C, Filip GA, David L, Moldovan B, Olteanu D, Clichici S, Baldea I (2023) Green synthesized gold and silver nanoparticles increased oxidative stress and induced cell death in colorectal adenocarcinoma cells. Nanomaterials 13(7):1251. https://doi.org/10.3390/nano13071251
40. Şirin MC, Cezaroğlu Y, Sesli Çetin E, Arıdoğan B, Trak D, Arslan Y (2023) Antibacterial and antibiofilm efficacy of colistin & meropenem conjugated silver nanoparticles against Escherichia coli and Klebsiella pneumoniae. J Basic Microbiol 63(12):1397–1411. https://doi.org/10.1002/jobm.202300219
41. Shankar SS, Ahmad A, Sastry M (2003) Geranium leaf assisted biosynthesis of silver nanoparticles. Biotechnol Prog 19(6):1627–1631. https://doi.org/10.1021/bp034070w
42. Rasheed T, Bilal M, Iqbal HMN, Li C (2017) Green biosynthesis of silver nanoparticles using leaves extract of Artemisia vulgaris and their potential biomedical applications. Colloids Surf B Biointerfaces 158:408–415. https://doi.org/10.1016/j.colsurfb.2017.07.011
43. Hassanisaadi M, Bonjar AHS, Rahdar A, Varma RS, Ajalli N, Pandey S (2022) Eco-friendly biosynthesis of silver nanoparticles using Aloysia citrodora leaf extract and evaluations of their bioactivities. Mater Today Commun 33:104183. https://doi.org/10.1016/j.mtcomm.2022.104183
44. Chakraborty B, Bhat MP, Basavarajappa DS, Rudrappa M, Nayaka S, Kumar RS, Perumal K (2023) Biosynthesis and characterization of polysaccharide-capped silver nanoparticles from Acalypha indica L. and evaluation of their biological activities. Environ Res 225:115614. https://doi.org/10.1016/j.envres.2023.115614
45. Alhomaidi E, Jasim SA, Amin HIM, Lima Nobre MA, Khatami M, Jalil AT, Hussain Dilfy S (2022) Biosynthesis of silver nanoparticles using Lawsonia inermis and their biomedical application. IET Nanobiotechnol 16(7–8):284–294. https://doi.org/10.1049/nbt2.12005
46. Katta VKM, Dubey RS (2021) Green synthesis of silver nanoparticles using Tagetes erecta plant and investigation of their structural, optical, chemical and morphological properties. Mater Today Proc. ;45:794–798. https://doi.org/10.1016/j.matpr.2021.01.102
47. Pal S, Tak YK, Song JM (2007) Does the antibacterial activity of silver nanoparticles depend on the shape of the nanoparticle? A study of the gram-negative bacterium Escherichia coli. Appl Environ Microbiol 73(6):1712–1720. https://doi.org/10.1128/AEM.02218-06
48. Mukherji S, Bharti S, Shukla G, Mukherji S (2019) Synthesis and characterization of size-and shape-controlled silver nanoparticles. Phys Sci Rev 4(1):20170082. https://doi.org/10.1515/psr-2017-0082

49. Hemmati S, Rashtiani A, Zangeneh MM, Mohammadi P, Zangeneh A, Veisi H (2019) Green synthesis and characterization of silver nanoparticles using Fritillaria flower extract and their antibacterial activity against some human pathogens. Polyhedron 158:8–14. https://doi.org/10.1016/j.poly.2018.10.058
50. Chinnappan S, Kandasamy S, Arumugam S, Seralathan KK, Thangaswamy S, Muthusamy G (2018) Biomimetic synthesis of silver nanoparticles using flower extract of Bauhinia purpurea and its antibacterial activity against clinical pathogens. Environ Sci Pollut Res 25:963–969. https://doi.org/10.1007/s11356-017-0585-9
51. Palithya S, Gaddam SA, Kotakadi VS, Penchalaneni J, Golla N, Krishna SBN, Naidu CV (2022) Green synthesis of silver nanoparticles using flower extracts of Aerva lanata and their biomedical applications. Part Sci Technol 40(1):84–96. https://doi.org/10.1080/02726351.2020.1864068
52. Mata R, Nakkala JR, Sadras SR (2015) Catalytic and biological activities of green silver nanoparticles synthesized from Plumeria alba (frangipani) flower extract. Mater Sci Eng C 51:216–225. https://doi.org/10.1016/j.msec.2015.02.035
53. Devanesan S, AlSalhi MS (2021) Green synthesis of silver nanoparticles using the flower extract of Abelmoschus esculentus for cytotoxicity and antimicrobial studies. Int J Nanomed 16:3343–3356. https://doi.org/10.2147/IJN.S305482
54. Gogoi N, Babu PJ, Mahanta C, Bora U (2015) Green synthesis and characterization of silver nanoparticles using alcoholic flower extract of Nyctanthes arbortristis and in vitro investigation of their antibacterial and cytotoxic activities. Mater Sci Eng C 46:463–469. https://doi.org/10.1016/j.msec.2014.10.063
55. Peron S, Hadi F, Azarbani F, Ananda Murthy HC (2021) Antimicrobial, antioxidant, anti-glycation and toxicity studies on silver nanoparticles synthesized using Rosa damascena flower extract. Green Chem Lett Rev 14(3):519–533. https://doi.org/10.1080/17518253.2021.1949168
56. Moteriya P, Chanda S (2017) Synthesis and characterization of silver nanoparticles using Caesalpinia pulcherrima flower extract and assessment of their in vitro antimicrobial, antioxidant, cytotoxic, and genotoxic activities. Artif Cells Nanomed Biotechnol 45(8):1556–1567. https://doi.org/10.1080/21691401.2017.1282491
57. Hajebi S, Tabrizi MH, Moghaddam MN, Shahraki F, Yadamani S (2019) Rapeseed flower pollen bio-green synthesized silver nanoparticles: A promising antioxidant, anticancer and antiangiogenic compound. JBIC J Biol Inorg Chem 24:395–404. https://doi.org/10.1007/s00775-019-01658-8
58. Varadavenkatesan T, Selvaraj R, Vinayagam R (2019) Dye degradation and antibacterial activity of green synthesized silver nanoparticles using Ipomoea digitata Linn. flower extract. Int J Environ Sci Technol 16:2395–2404. https://doi.org/10.1007/s13762-018-2107-9
59. Otari SV, Patil RM, Nadaf NH, Ghosh SJ, Pawar SH (2012) Green biosynthesis of silver nanoparticles from an actinobacteria Rhodococcus sp. Mater Lett 72:92–94. https://doi.org/10.1016/j.matlet.2011.07.026

60. Ajitha B, Reddy YAK, Reddy PS (2014) Biosynthesis of silver nanoparticles using Plectranthus amboinicus leaf extract and its antimicrobial activity. Spectrochim Acta Mol Biomol Spectrosc 128:257–262. https://doi.org/10.1016/j.saa.2014.03.048
61. Kaman PK, Dutta P (2019) Synthesis, characterization and antifungal activity of biosynthesized silver nanoparticle. Indian Phytopathol 72:79–88. https://doi.org/10.1007/s42360-018-0075-7
62. Singhal G, Bhavesh R, Kasariya K, Sharma AR, Singh RP (2011) Biosynthesis of silver nanoparticles using Ocimum sanctum (Tulsi) leaf extract and screening its antimicrobial activity. J Nanopart Res 13:2981–2988. https://doi.org/10.1007/s11051-011-0369-7
63. Pourmortazavi SM, Taghdiri M, Makari V, Rahimi-Nasrabadi M (2015) Procedure optimization for green synthesis of silver nanoparticles by aqueous extract of Eucalyptus oleosa. Spectrochim Acta Mol Biomol Spectrosc 136:1249–1254. https://doi.org/10.1016/j.saa.2014.10.017
64. Ali F, Younas U, Nazir A, Hassan F, Iqbal M, Mukhtar S, Ishfaq A (2022) Biosynthesis and characterization of silver nanoparticles using strawberry seed extract and evaluation of their antibacterial and antioxidant activities. J Saudi Chem Soc 26(6):101558. https://doi.org/10.1016/j.jscs.2022.101558
65. Hemlata, Meena PR, Singh AP, Tejavath KK (2020) Biosynthesis of silver nanoparticles using Cucumis prophetarum aqueous leaf extract and their antibacterial and antiproliferative activity against cancer cell lines. ACS Omega 5(10):5520–5528. https://doi.org/10.1021/acsomega.0c00602
66. Sriranjani R, Srinithya B, Vellingiri V, Brindha P, Anthony SP, Sivasubramanian A, Muthuraman MS (2016) Silver nanoparticle synthesis using Clerodendrum phlomidis leaf extract and preliminary investigation of its antioxidant and anticancer activities. J Mol Liq 220:926–930. https://doi.org/10.1016/j.molliq.2016.05.011
67. Badmus JA, Oyemomi SA, Adedosu OT, Yekeen TA, Azeez MA, Adebayo EA, Marnewick JL (2020) Photo-assisted bio-fabrication of silver nanoparticles using Annona muricata leaf extract: exploring the antioxidant, anti-diabetic, antimicrobial, and cytotoxic activities. Heliyon 6(11):e05515. https://doi.org/10.1016/j.heliyon.2020.e05515
68. Khuda F, Jamil M, Khalil AAK, Ullah R, Ullah N, Naureen F, Ahn MJ (2022) Assessment of antioxidant and cytotoxic potential of silver nanoparticles synthesized from root extract of Reynoutria japonica Houtt. Arab J Chem 15(12):104327. https://doi.org/10.1016/j.arabjc.2022.104327
69. Adebayo AE, Oke AM, Lateef A, Oyatokun AA, Abisoye OD, Adiji IP, Abbas SH (2019) Biosynthesis of silver, gold and silver–gold alloy nanoparticles using Persea americana fruit peel aqueous extract for their biomedical properties. Nanotechnol Environ Eng 4(1):13. https://doi.org/10.1007/s41204-019-0067-9
70. Kaviya S, Santhanalakshmi J, Viswanathan B, Muthumary J, Srinivasan K (2011) Biosynthesis of silver nanoparticles using Citrus sinensis peel extract and its antibacterial activity. Spectrochim Acta Mol Biomol Spectrosc 79(3):594–598. https://doi.org/10.1016/j.saa.2011.03.057

71. Murugan K, Senthilkumar B, Senbagam D, Al-Sohaibani S (2014) Biosynthesis of silver nanoparticles using Acacia leucophloea extract and their antibacterial activity. Int J Nanomed 9:2431–2438. https://doi.org/10.2147/IJN.S59660
72. Timotina M, Aghajanyan A, Schubert R, Trchounian K, Gabrielyan L (2022) Biosynthesis of silver nanoparticles using extracts of Stevia rebaudiana and evaluation of antibacterial activity. World J Microbiol Biotechnol 38(11):196. https://doi.org/10.1007/s11274-022-03387-8
73. Qamer S, Romli MH, Che-Hamzah F, Misni N, Joseph NMS, Al-Haj NA, Amin-Nordin S (2021) Systematic review on biosynthesis of silver nanoparticles and antibacterial activities: Application and theoretical perspectives. Molecules 26(16):5057. https://doi.org/10.3390/molecules26165057

Figures

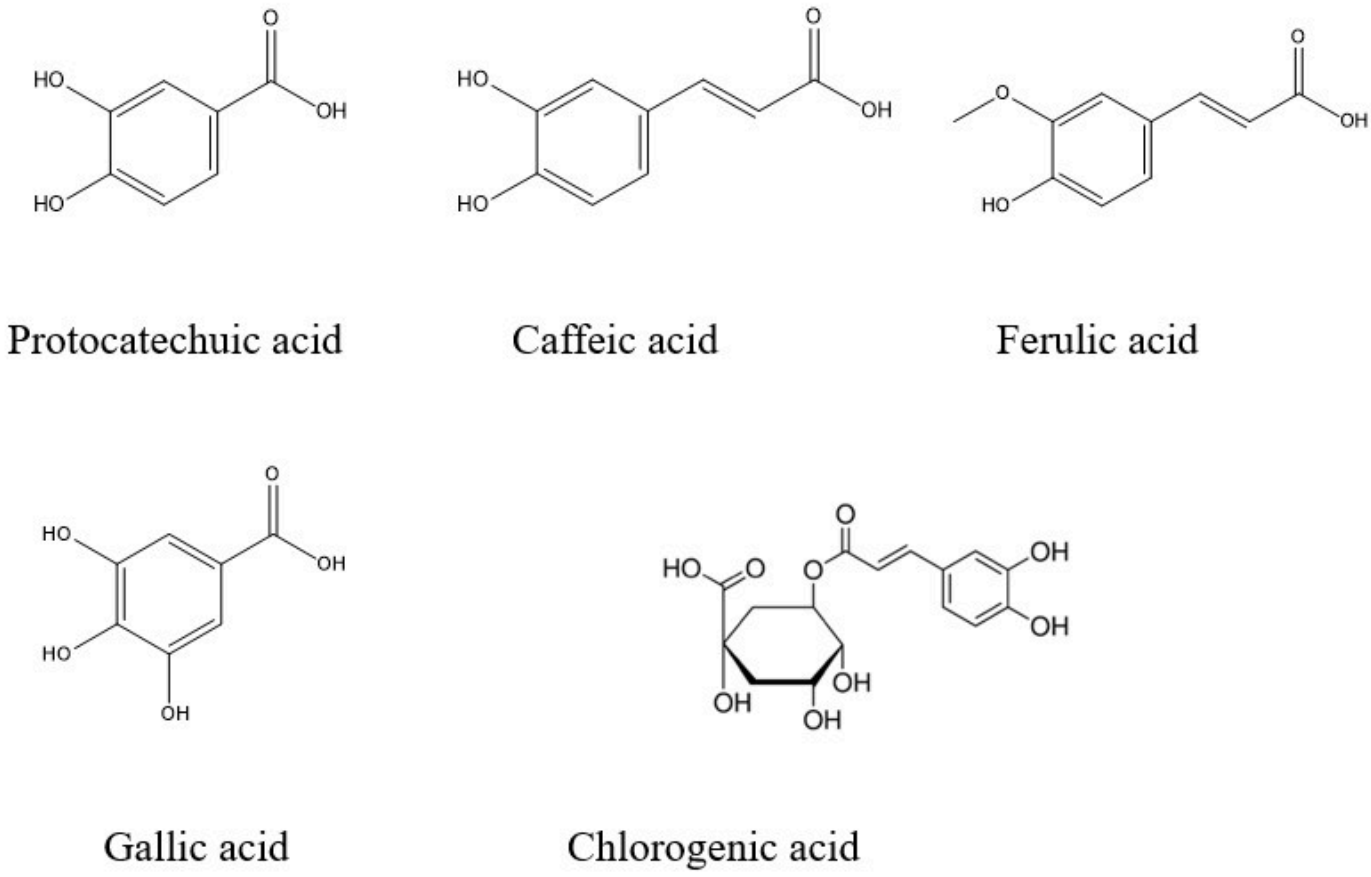

Figure 1

Some polyphenol structures found in *the Leucas lanata* plant

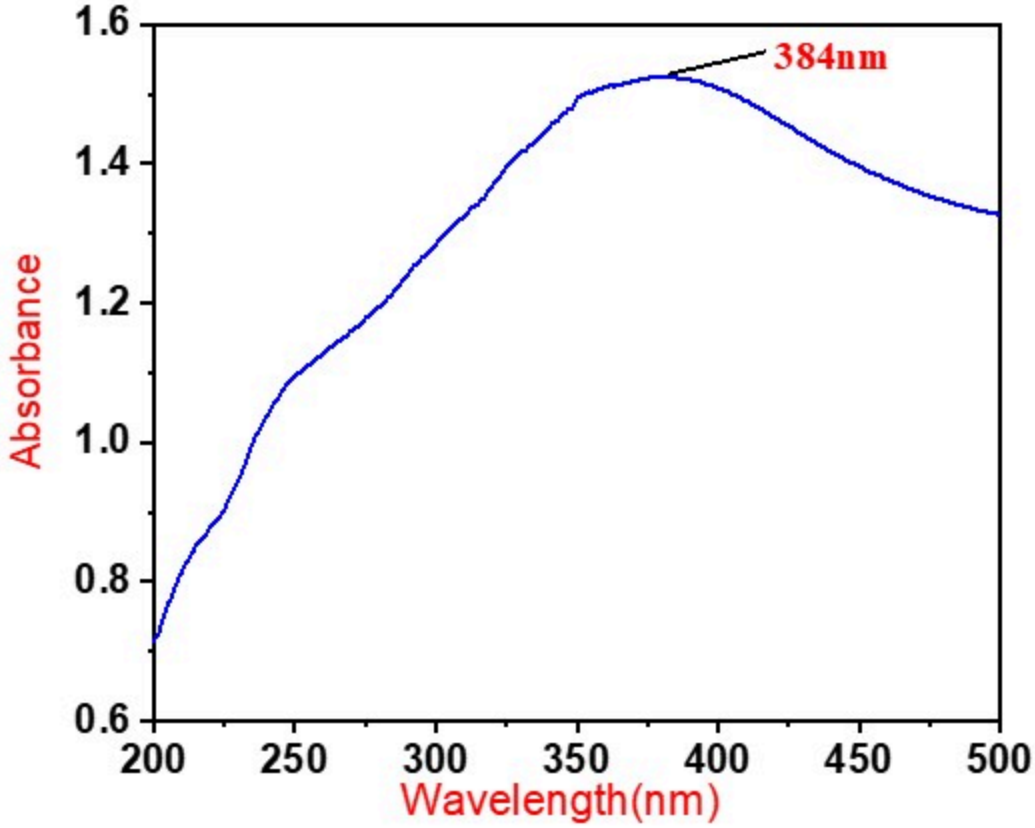

Figure 2

UV-VIS (Ultraviolet-Visible) spectra for synthesized AgNPs

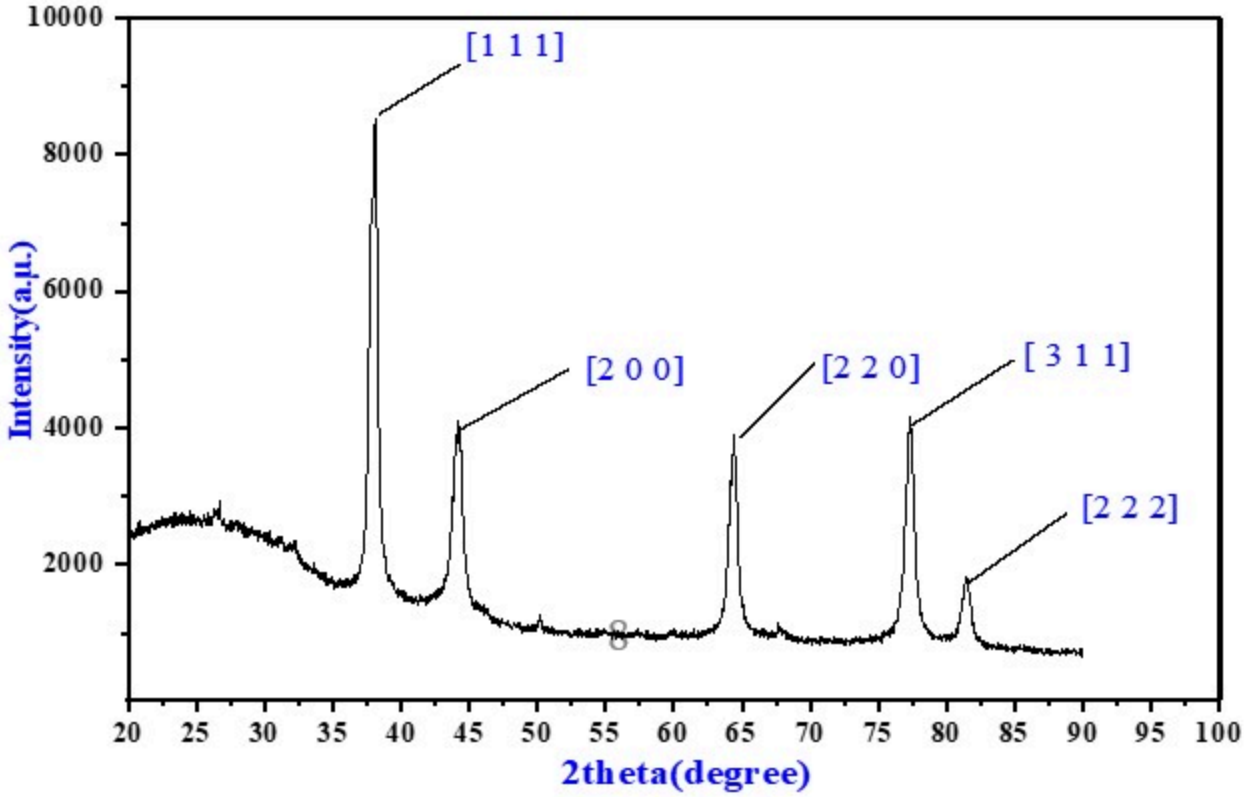

Figure 3

X-ray beam diffraction pattern of synthesized AgNPs

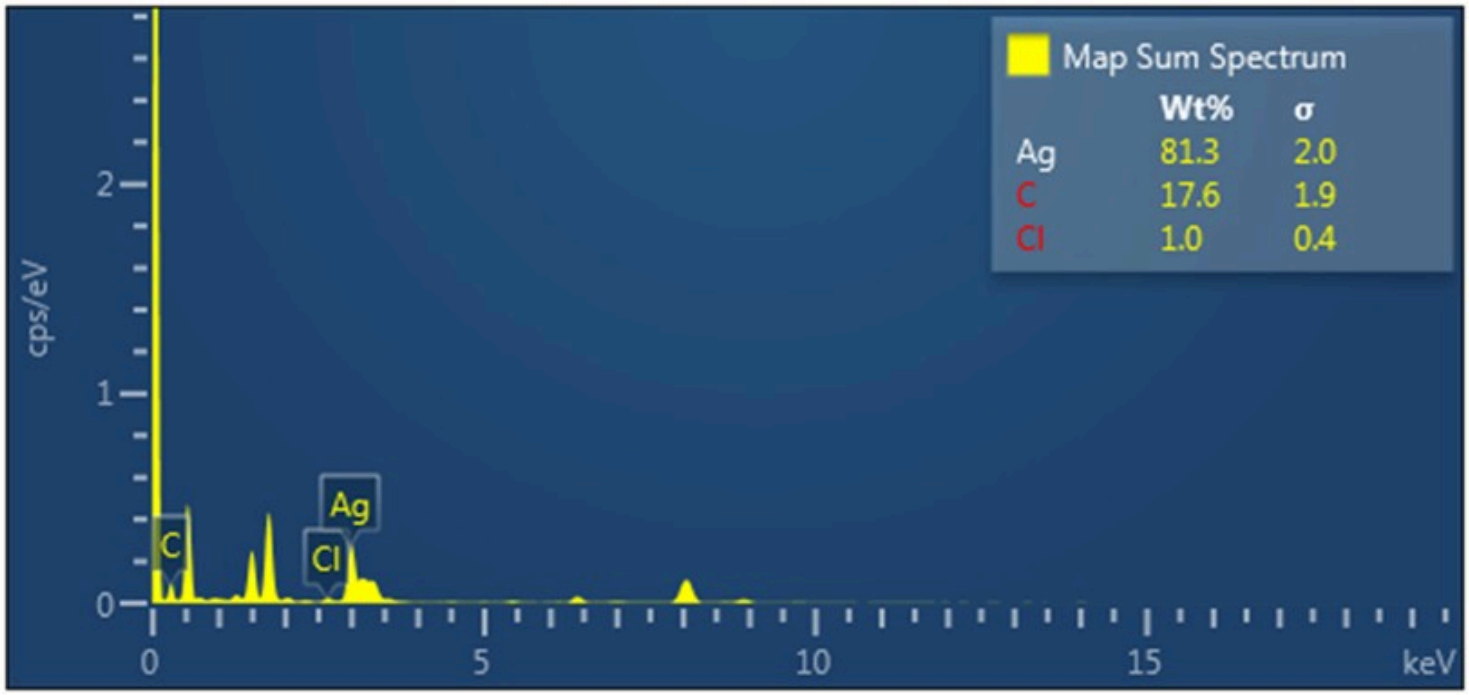

Figure 4

EDAX (Energy Dispersive X-ray) spectra showing the elemental composition of L-AgNPs

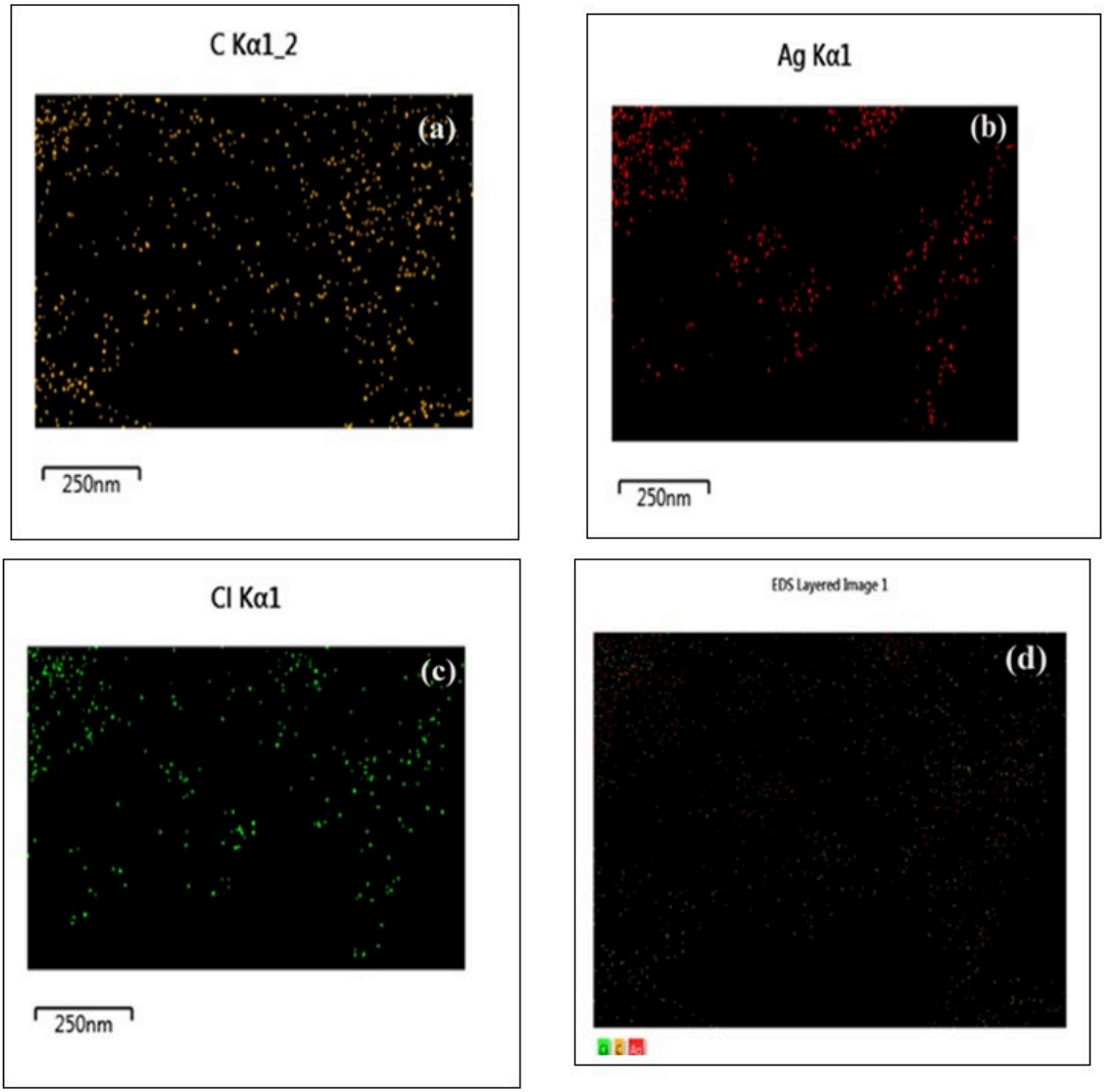

Figure 5

EDAX (Energy Dispersive X-ray) Element mapping of green synthesized L-AgNPs

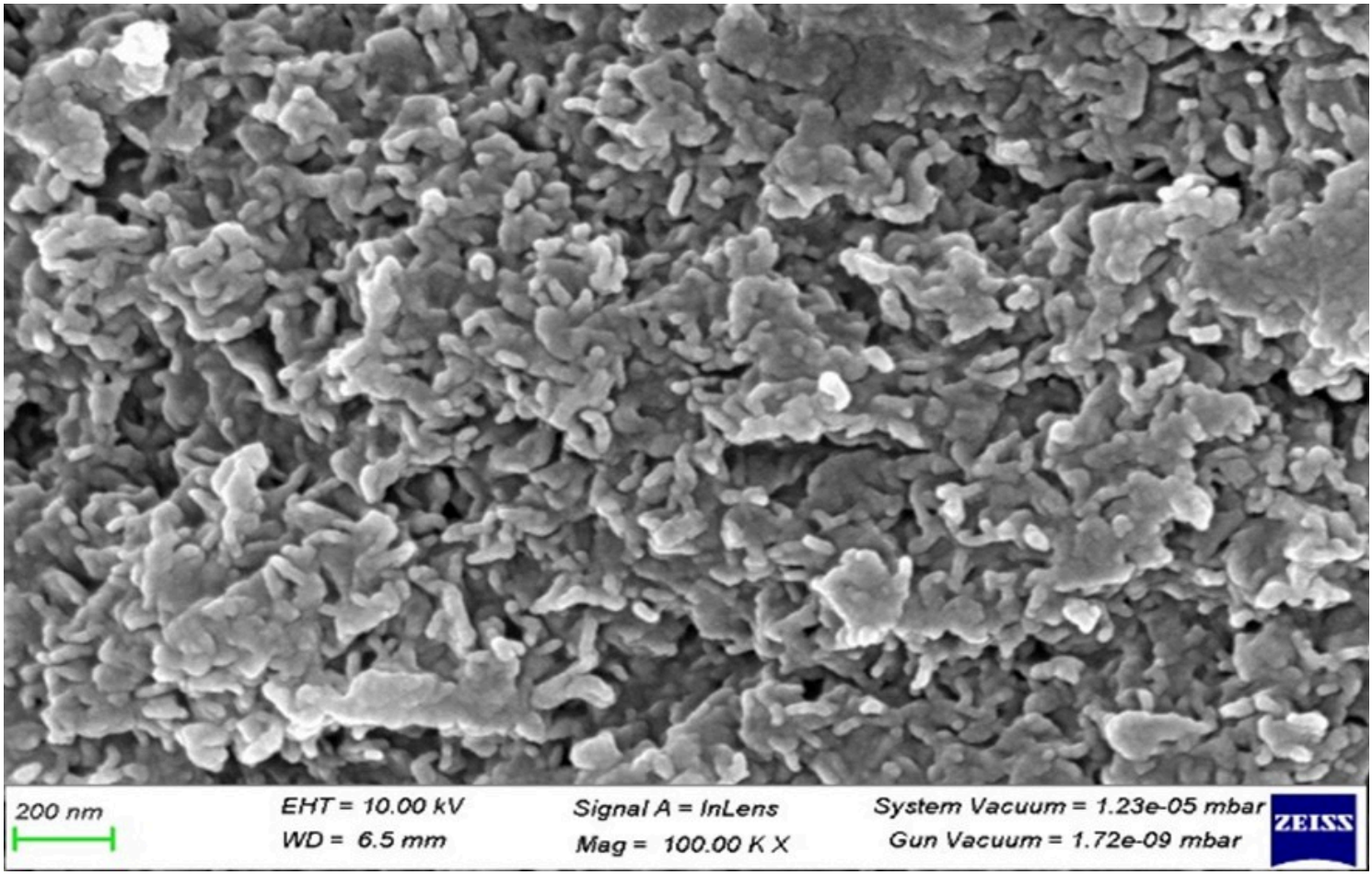

Figure 6

Field emission scanning electron microscopy image for synthesized L-AgNPs

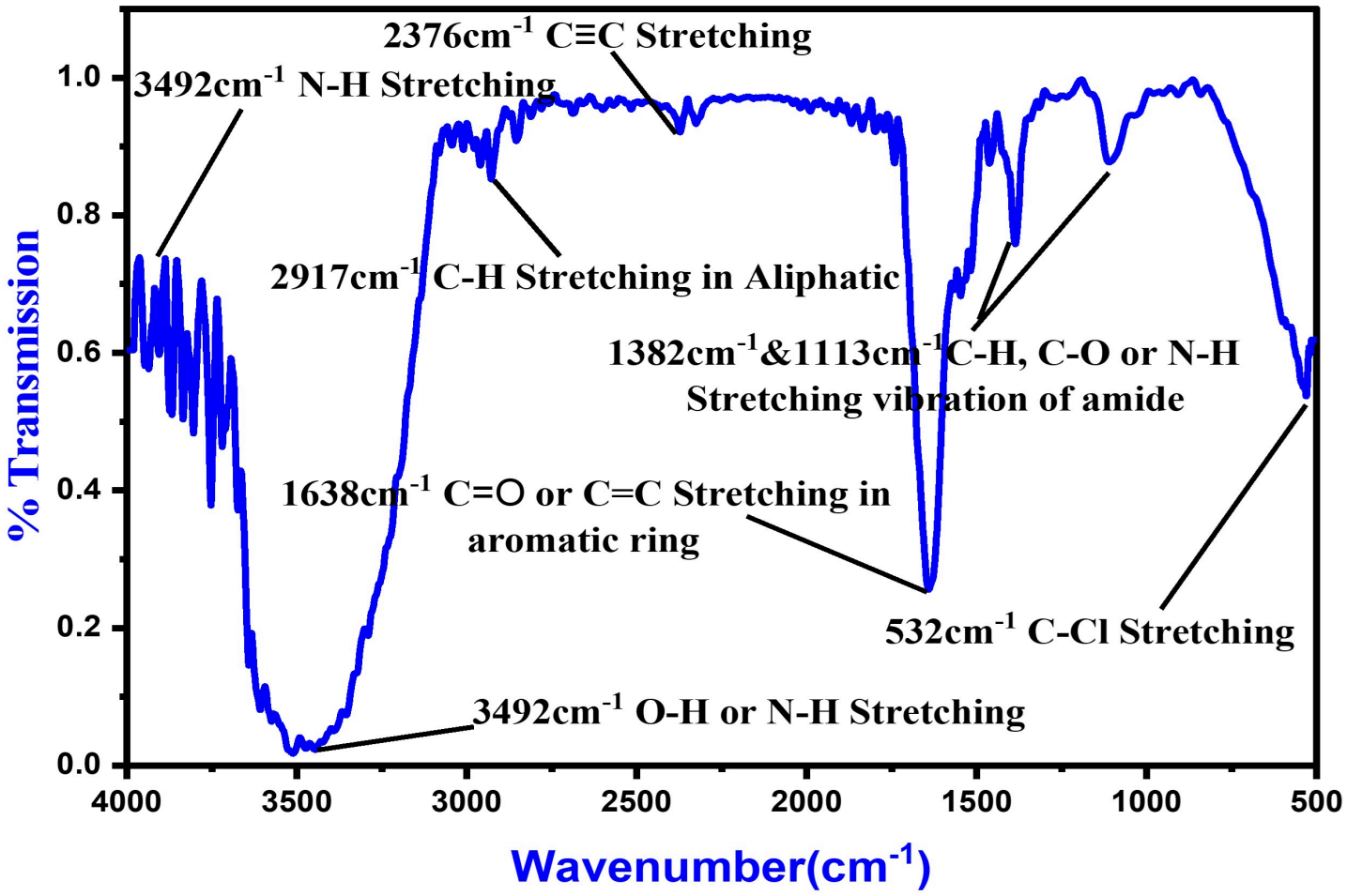

Figure 7

FT-IR spectra of synthesized AgNPs

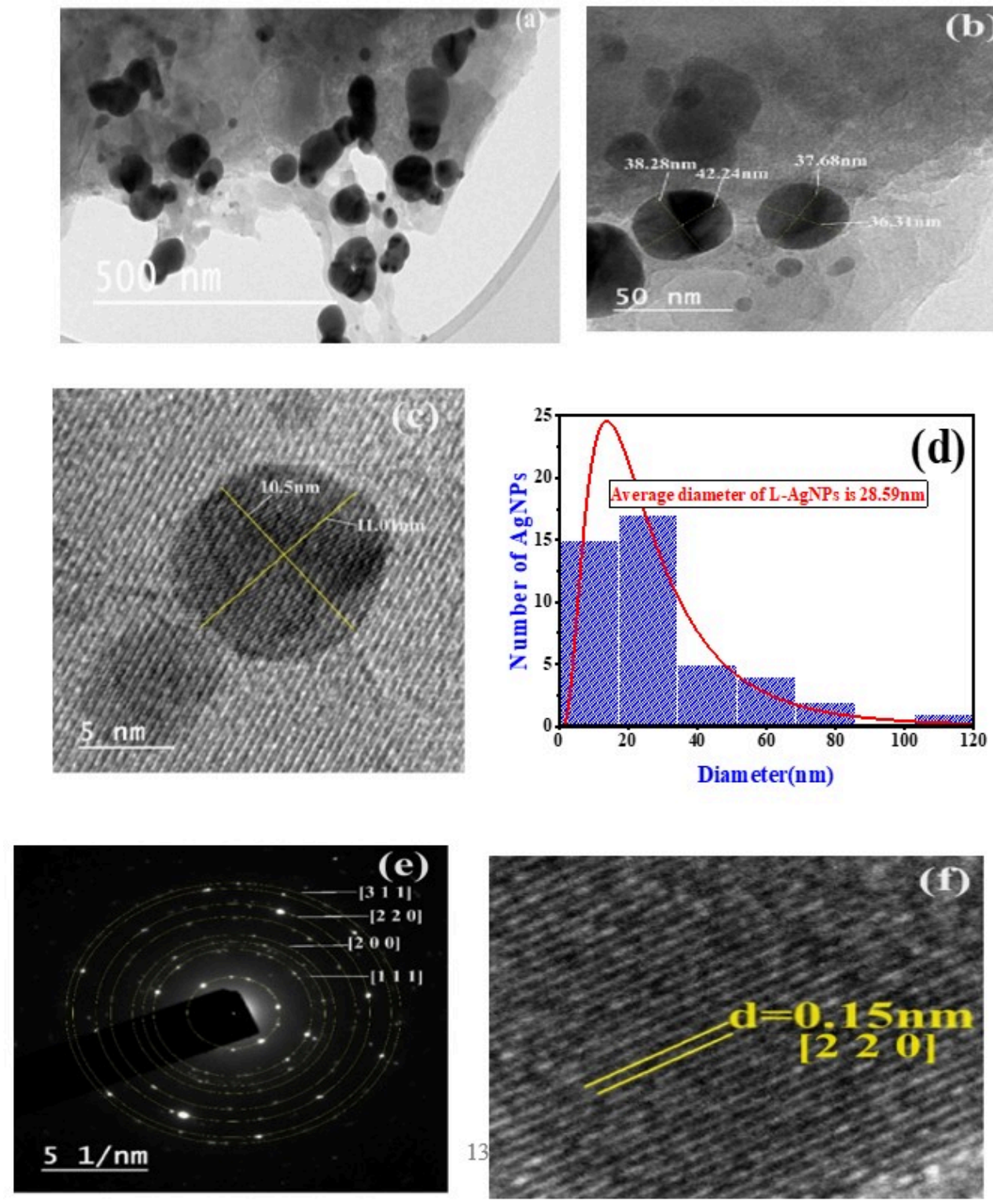

Figure 8

(a) HRTEM Image at high magnification, (b,c) Particle size of L-AgNPs, (d) Particle size distribution of biosynthesized AgNPs,(e) SAED (Selected area electron diffraction) patterns of the synthesized L-AgNPs, (f) d spacing value for [2 0 0] plane.

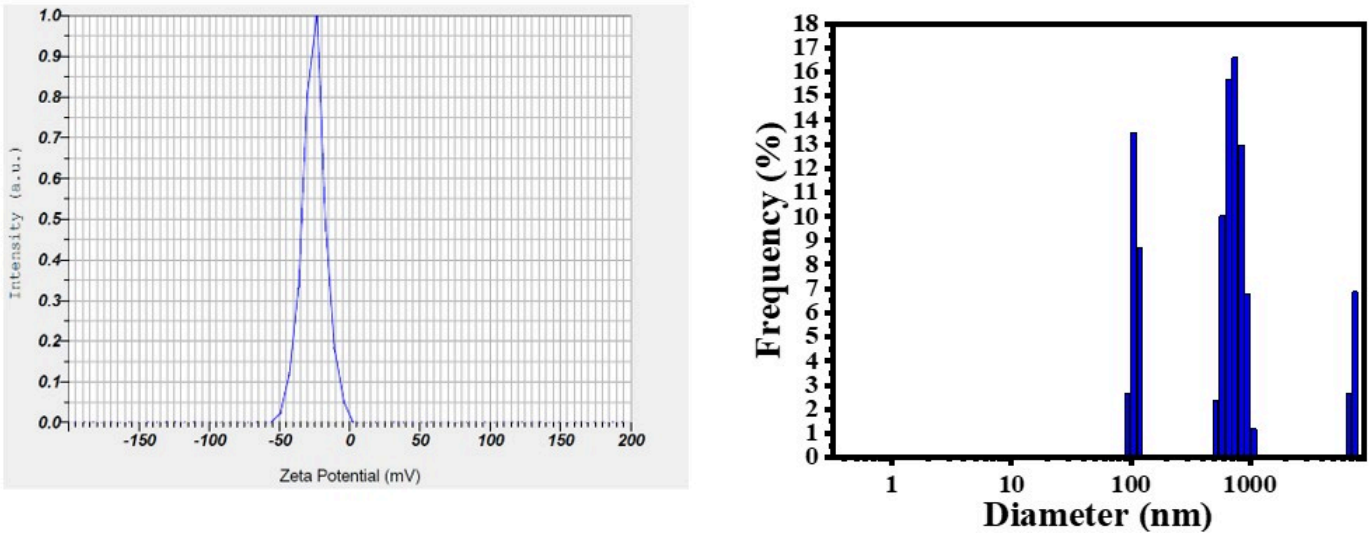

Figure 9

Zeta potential of L-AgNPS (a) and Particle size distribution (b)

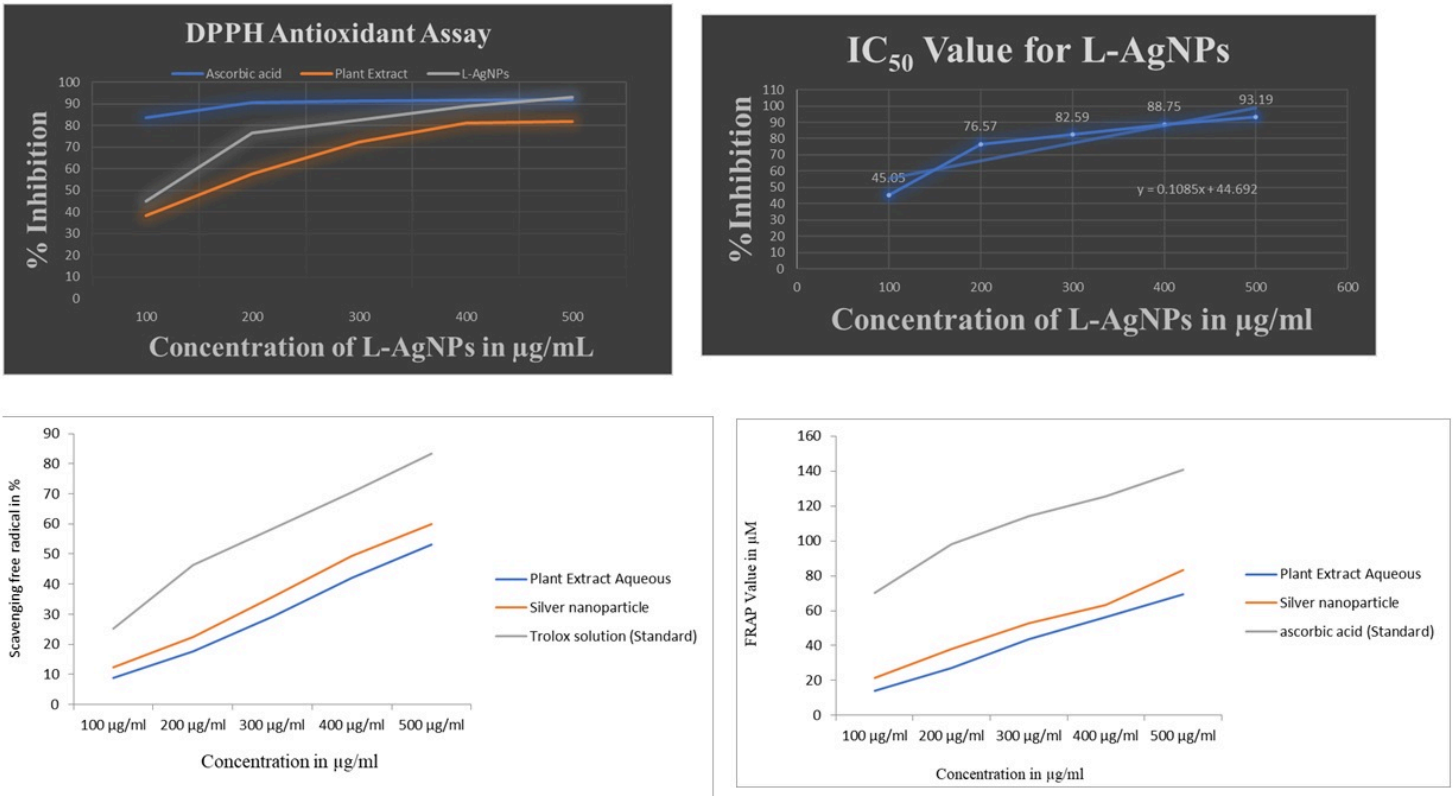

Figure 10

(a): DPPH (2,2-Diphenyl-1-picrylhydrazyl) assay analysis for Antioxidant activity

(b): DPPH (2,2-Diphenyl-1-picrylhydrazyl) Free radical scavenging Activity AgNPs and IC_{50} values

(c): **Plant extract (aqueous solution) and Silver nanoparticle ABTS assay with standard**

(d): Plant extract (aqueous solution) and silver nanoparticle FRAP assay (µM) with standard

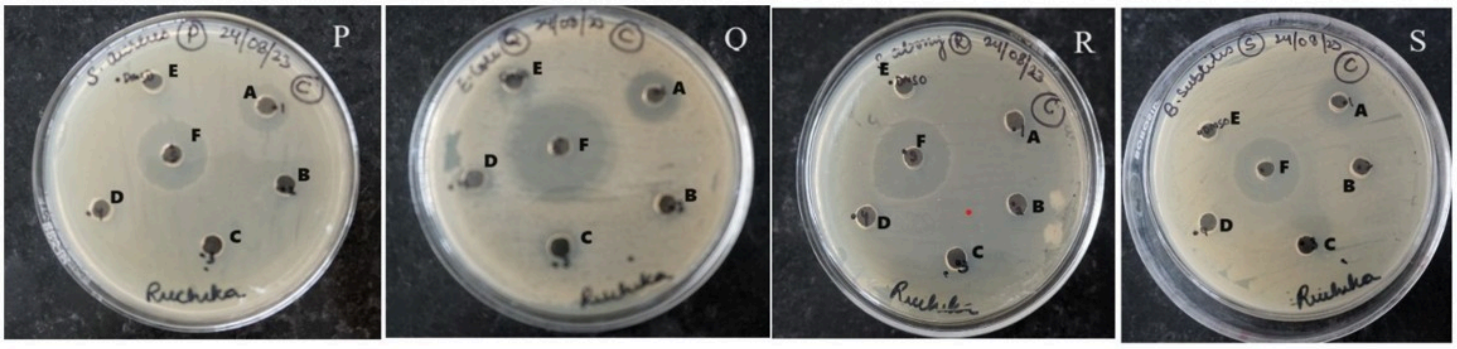

Figure 11

Inhibition Zone of *Leucas lanata* extract against different Bacteria (P-*Staphylococcus aureus*; Q-*Escherichia coli*; R- *Salmonella abony*; S- *Bacillus subtilis*)

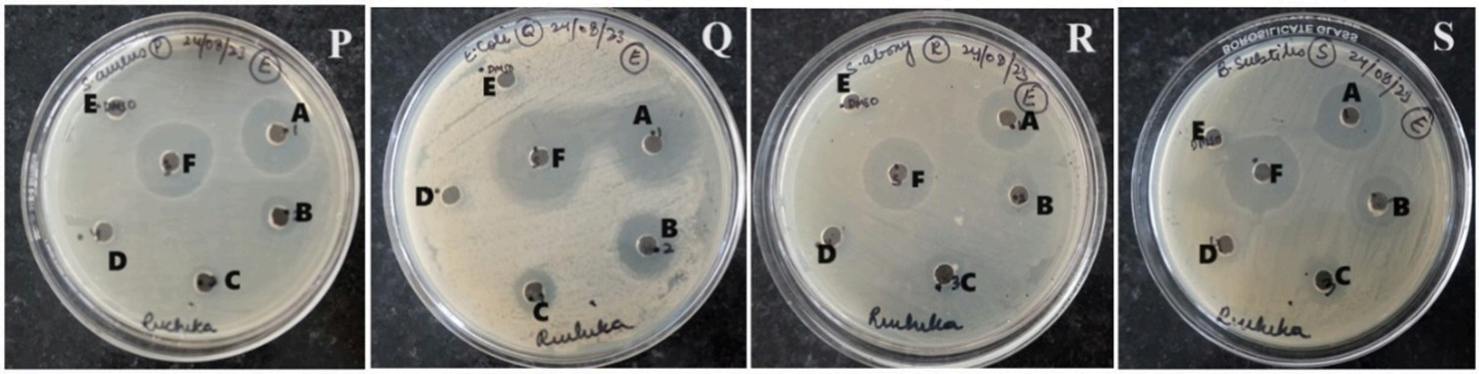

Figure 12

Inhibition Zone of L- AgNPs against different Bacteria (P- *Staphylococcus aureus*; Q- *Escherichia coli*; R-*Salmonella abony*; S- *Bacillus subtilis*)

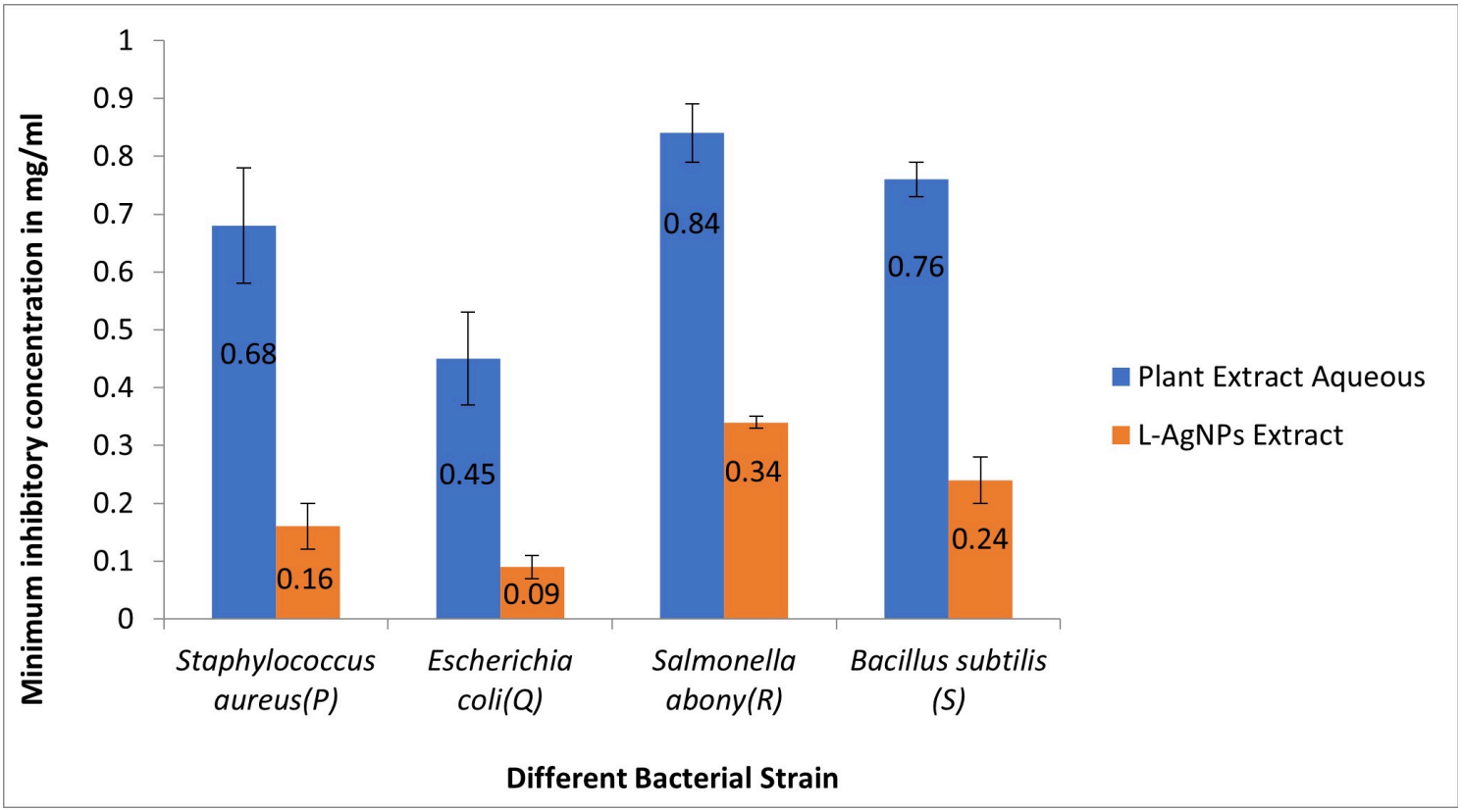

Figure 13

The MIC of plant extract and L- AgNPs against different bacterial strains

Supplementary Files

This is a list of supplementary files associated with this preprint. Click to download.

- floatimage1.png